

Anomalous Hall Effect in a Two Dimensional Electron Gas with Magnetic Impurities

Tamara S. Nunner,¹ Gergely Zaránd,² and Felix von Oppen¹

¹*Institut für Theoretische Physik, Freie Universität Berlin, Arnimallee 14, 14195 Berlin, Germany*

²*Institute of Physics, Technical University Budapest, Budapest, H-1521, Hungary*

(Received 24 November 2007; published 11 June 2008)

Magnetic impurities play an important role in many spintronics-related materials. Motivated by this fact, we study the anomalous Hall effect in the presence of magnetic impurities, focusing on two-dimensional electron systems with Rashba spin-orbit coupling. We find a highly nonlinear dependence on the impurity polarization, including possible sign changes. At small impurity magnetizations, this is a consequence of the remarkable result that the linear term is independent of the spin-orbit coupling strength. Near saturation of the impurity spins, the anomalous Hall conductivity can be resonantly enhanced, due to interference between potential and magnetic scattering.

DOI: 10.1103/PhysRevLett.100.236602

PACS numbers: 72.15.Gd, 72.20.Dp, 72.25.-b, 85.75.-d

Introduction.—In ferromagnetic materials, the Hall resistance acquires an anomalous contribution that is proportional to the magnetization of the sample [1–3]. Although this anomalous Hall effect (AHE) has become a standard tool to determine the magnetization of ferromagnets and has been known for more than a century, its mechanism is still under debate. The interest in the origin of the AHE has recently been renewed due to its close relation to the spin Hall effect. Particular attention has been paid to intrinsic mechanisms [1] based on the Berry phase, which can arise when the spin-orbit interaction modifies the band structure. This is in contrast to extrinsic mechanisms [2–4], which require the presence of impurities for the occurrence of an anomalous Hall effect. Surprising results have been found even for simple systems such as a two-dimensional electron gas (2DEG) with Rashba spin-orbit interaction where it turns out that in the presence of pointlike potential disorder the AHE vanishes when both of the spin-split bands are occupied [5–11].

So far, most treatments of the AHE have only considered the presence of potential impurities. However, in many materials, which are of interest for spintronics applications such as diluted magnetic semiconductors, magnetic impurities play a fundamental role. Although extrinsic mechanisms for the AHE based on scattering by magnetic impurities have been suggested [12], little is known about the influence of magnetic impurities in materials with strong spin-orbit interaction, where the AHE is induced by intrinsic mechanisms. To learn about the role of magnetic impurities, we avoid the complexities of realistic band structures and instead provide a thorough analysis of a simple model: a 2DEG with Rashba spin-orbit interaction where the presence of magnetic impurities is known to induce a finite AHE even when both spin-split bands are occupied [9]. We find that surprisingly rich physics emerges even in this model system.

We expect that our model can be tested experimentally in magnetically doped 2DEGs [13], once they are produced with asymmetric confinement potentials. This may be realized in heterojunctions made of a material with large

spin-orbit coupling. At present, a robust AHE has been observed in a magnetically doped 2DEG with *weak* spin-orbit coupling, based on a modulation-doped quantum well of $\text{Zn}_{1-x-y}\text{Cd}_y\text{Mn}_x\text{Se}$ ($x \sim 0.02$, $y \sim 0.12$) sandwiched between ZnSe barriers [14].

To model a magnetically doped 2DEG with Rashba spin-orbit coupling, we use the Hamiltonian

$$H = \frac{\mathbf{p}^2}{2m} + \alpha \boldsymbol{\sigma} \cdot (\mathbf{p} \times \hat{z}) + \sum_i [V + JS_i \cdot \boldsymbol{\sigma}] \delta(\mathbf{r} - \mathbf{R}_i). \quad (1)$$

Here, α denotes the strength of the spin-orbit interaction. The impurities at positions \mathbf{R}_i affect the conduction electrons through a potential $V\delta(\mathbf{r} - \mathbf{R}_i)$ and an exchange coupling $JS_i \cdot \boldsymbol{\sigma}$. (Here, \mathbf{S}_i denotes the impurity and $\boldsymbol{\sigma}$ the electron spin.) Note that we average only over the positions of the impurity atoms whereas the potential parameters V and J are the same for all impurities. Thus our treatment does not correspond to a white noise approximation. Our analysis below includes interference of amplitudes from potential and magnetic scattering, and accounts for all significant contributions to the AHE, including skew scattering. Remarkably, we find that the AHE deviates significantly from the conventional linear magnetization dependence except for the region of very small polarization of the impurity spins. For strong impurity polarization, we obtain a resonant behavior of the anomalous Hall conductivity. This enhancement arises from an interference-induced suppression of the scattering rate for the minority carriers.

Anomalous Hall conductivity.—Our theory is based on the Streda-Kubo approach, which decomposes the Hall conductivity $\sigma_{yx} = \sigma_{yx}^I + \sigma_{yx}^{II}$ into a Fermi-surface contribution σ_{yx}^I and a contribution σ_{yx}^{II} from the entire Fermi sea [15,16]. In our model the AHE is dominated by the Fermi-surface contribution

$$\sigma_{yx}^I = -\frac{e^2}{2\pi V} \text{Tr}[v_y G_{\epsilon_F}^R v_x G_{\epsilon_F}^A], \quad (2)$$

where $G^{R,A}$ denotes the retarded and advanced Green

functions and the velocity operators are given by $v_{x,y} = p_{x,y}/m \mp \alpha \sigma_{y,x}$. Since the contributions of $G^R G^R$ and $G^A G^A$ are of higher order in the disorder scattering rate Γ [17], they have already been omitted in Eq. (2). Regarding σ_{yx}^I it is known that it vanishes for $\epsilon_F > h$ in clean systems [11], where h is the effective magnetic field. This remains true also in the presence of magnetic impurities as long as vertex corrections are neglected, which contribute only to higher order in Γ [17].

To compute the anomalous Hall conductivity, we treat the exchange interaction at a mean-field level, average over the impurity positions, and incorporate disorder effects perturbatively. Within the mean-field approximation, the exchange interaction leads to an additional internal Zeeman field acting on the electrons, which is typically larger than the applied magnetic field h_{ext} . Thus, the electrons are subject to an average effective Zeeman field $h \simeq \epsilon_J \langle S_z \rangle / S$, where $\epsilon_J = n_i J S$ is the maximal exchange field and n_i denotes the concentration of impurities. At mean-field level, the nonzero impurity-spin expectation values are given by $\langle S_z \rangle = -\partial \ln Z / \partial (\beta \tilde{h})$, $\langle S_z^2 \rangle = (1/Z) \partial^2 Z / \partial (\beta \tilde{h})^2$ with the Brillouin partition function $Z = \sinh[\beta J \tilde{h} (2S + 1)/2] / \sinh(\beta \tilde{h}/2)$ and the effective field $\tilde{h} = n J \langle \sigma \rangle$ acting on the impurity spins. Here, n and $\langle \sigma \rangle$ denote the density and polarization of the electrons. Instead of calculating $\langle S_z \rangle$ self-consistently, we treat it as a *parameter* which also determines the impurity-spin fluctuation $\langle S_z^2 \rangle$ within this mean-field approach.

Let us now consider the effects of disorder. In the mean-field approximation, the dispersion of the two subbands is given by $E_{k,\pm} = k^2/2m \pm \lambda_k$ with $\lambda_k = \sqrt{h^2 + \alpha^2 k^2}$, and the retarded Green function takes the form $G^{0,R} = G_0^{0,R} + \sum_{i=x,y,z} G_i^{0,R} \sigma_i$ with

$$\begin{aligned} G_0^{0,R} &= \frac{1}{2}(G_+^{0,R} + G_-^{0,R}), & G_z^{0,R} &= -\frac{h}{2\lambda_p}(G_+^{0,R} - G_-^{0,R}), \\ G_{x/y}^{0,R} &= \pm \frac{\alpha p_{y/x}}{2\lambda_p}(G_+^{0,R} - G_-^{0,R}), & G_{\pm}^{0,R} &= \frac{1}{\omega - E_{p_{\pm}} + i0^+}. \end{aligned} \quad (3)$$

Deriving the retarded self-energy of the 2DEG within the Born approximation, we obtain $\Sigma^R = -i(\Gamma + \Gamma_z \sigma_z)$ with $\Sigma^R = -\frac{in_i}{4} \{ [V^2 + J^2 S(S+1) + 2VJ \langle S_z \rangle \sigma_z] K_1 - [2VJ \langle S_z \rangle + \{V^2 + J^2 [2 \langle S_z^2 \rangle - S(S+1)] \} \sigma_z] h K_2 \}$. (4)

Here, $K_1 = (\nu_+ + \nu_-)$ and $K_2 = \nu_+/\lambda_+ - \nu_-/\lambda_-$ where $\nu_{\pm} = m\lambda_{\pm}/\sqrt{h^2 + 2\epsilon_{\text{so}}\epsilon_F + (\epsilon_{\text{so}})^2}$ with $\epsilon_{\text{so}} = \alpha^2 m$ is related to the density of states of the two bands at the Fermi energy ϵ_F and $\lambda_{\pm} = \lambda_{k_{\pm}}$ with k_{\pm} being the corresponding Fermi wave vectors. If only pointlike potential scatterers are present and scattering from magnetic impurities is neglected, the anomalous Hall conductivity vanishes except for the extreme limit $\epsilon_F < h$. Here, we focus on the more realistic regime of $\epsilon_F > h$ where *both* subbands are

partially occupied and where it is the magnetic impurities which induce a nonzero anomalous Hall effect.

When both subbands are occupied, one finds $K_2 = 0$ and hence a significant simplification of the self-energy in Eq. (4). The impurity averaged Green function also takes the form of Eq. (3), with the replacements $E \rightarrow E + i\Gamma$ and $h \rightarrow h + i\Gamma_z$. In the following, we assume weak disorder scattering in the sense $\Gamma_z \ll \lambda_p$, such that

$$G_{\pm}^R \simeq \frac{1}{\omega - E_{p_{\pm}} + i\Gamma_{\pm}}, \quad \Gamma_{\pm} = \Gamma \mp \Gamma_z \frac{h}{\lambda_{\pm}}. \quad (5)$$

The anomalous Hall conductivity σ_{yx}^I can now be computed as the sum of the ladder diagrams $\sigma_{yx}^{I,l}$ [see Fig. 1(a)] and the skew-scattering contribution $\sigma_{yx}^{I,s}$ [see Fig. 1(b)]. Using $n_i \tilde{V}^2 = n_i (V^2 - J^2 \langle S_z^2 \rangle)$, a lengthy but standard evaluation of the diagrams yields $\sigma_{yx}^I = \sigma_{yx}^{I,l} + \sigma_{yx}^{I,s}$ with

$$\begin{aligned} \sigma_{yx}^{I,l} &= \frac{e^2}{2\pi} 2\alpha(\gamma_1 + iI_3) \\ &\quad - \frac{e^2 n_i \tilde{V}^2 [2\gamma_1 \gamma_2 (1 - n_i \tilde{V}^2 I_1) + in_i \tilde{V}^2 I_2 (\gamma_2^2 - \gamma_1^2)]}{\pi (1 - n_i \tilde{V}^2 I_1)^2 - (n_i \tilde{V}^2 I_2)^2}, \\ \sigma_{yx}^{I,s} &= \frac{e^2 2n_i m J \langle S_z \rangle [V^2 - J^2 S(S+1)] \gamma_2^2}{2\pi (1 - n_i \tilde{V}^2 I_1)^2} \end{aligned} \quad (6)$$

where

$$\gamma_1 = i(I_3 - \alpha I_2), \quad \gamma_2 = I_4 - \alpha I_1 \quad (7)$$

and

$$\begin{aligned} I_1 &\approx \frac{1}{8} \left[\left(1 - \frac{h^2}{\lambda_+^2}\right) \frac{\nu_+}{\Gamma_+} + \left(1 - \frac{h^2}{\lambda_-^2}\right) \frac{\nu_-}{\Gamma_-} \right], \\ I_2 &\approx -\frac{i}{4} \left(\frac{\nu_+ h}{\lambda_+^2} + \frac{\nu_- h}{\lambda_-^2} - \frac{\Gamma_z}{\Gamma_+} \frac{\nu_+ \alpha^2 k_+^2}{\lambda_+^3} + \frac{\Gamma_z}{\Gamma_-} \frac{\nu_- \alpha^2 k_-^2}{\lambda_-^3} \right), \\ I_3 &\approx -\frac{i}{4} \alpha \Gamma_z \left[\frac{\nu_+}{\Gamma_+ \lambda_+} \left(\frac{\epsilon_F}{\lambda_+} - 1 \right) + \frac{\nu_-}{\Gamma_- \lambda_-} \left(\frac{\epsilon_F}{\lambda_-} + 1 \right) \right], \\ I_4 &\approx -\frac{1}{4} \alpha \left[\epsilon_F \left(\frac{\nu_+}{\Gamma_+ \lambda_+} - \frac{\nu_-}{\Gamma_- \lambda_-} \right) - \left(\frac{\nu_+}{\Gamma_+} + \frac{\nu_-}{\Gamma_-} \right) \right]. \end{aligned} \quad (8)$$

Here we have taken the weak scattering limit of $\sigma_{yx}^{I,s}$. As a result of several cancellations these expressions turn out to be formally similar to the ones of Ref. [11], derived for purely potential scatterers. The main differences are that

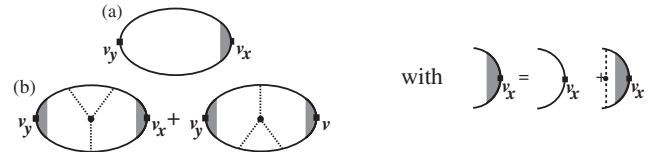


FIG. 1. Anomalous Hall conductivity: (a) ladder and (b) skew-scattering contributions. In analogy to Refs. [10,11] we consider for skew scattering only diagrams with a single third order impurity vertex and both external current vertices renormalized by ladder type vertex corrections. Since $\sigma_{yx}^{II} = 0$ in the parameter regime considered here, only diagrams for σ_{yx}^I are depicted.

additional terms proportional to $\langle S_z \rangle$ appear in the self-energy and that $n_i V^2$ is replaced by $n_i \tilde{V}^2$ in the vertex corrections. Furthermore, V^2 is replaced by $V^2 - J^2 S(S+1)$ in the numerator of the skew-scattering contribution.

We remark that the expression for the ladder contribution reduces to the results of Inoue *et al.* [9]: i.e., $\sigma_{yx}^{I,l} \approx e^2 \epsilon_{so} \epsilon_F^2 \delta^2 / (2\pi \hbar^3)$ with $\delta = \Gamma_z / \Gamma \approx 2J \langle S_z \rangle / V$, when taking the special limit of small spin-orbit interaction, large Fermi energy $\Delta_{so} \ll \hbar \ll \epsilon_F$ with $\Delta_{so} = \alpha k_F$, as well as small exchange component of the impurity potential. Here, however, we focus on the remarkably rich behavior of the anomalous Hall conductivity beyond this special limit. Although our treatment is set up for quantum spins, we shall restrict most formulas to classical spins. The corresponding expressions for quantum spins are similar but more complicated. We do, however, include the results for quantum spins in the figures.

Mechanisms.—Our model Eq. (1) contains the spin-orbit interaction only in the band structure. Several mechanisms contribute to the anomalous Hall conductivity, such as the Berry-phase, the skew-scattering, and the side-jump contributions. Our diagrammatic results properly capture *all of these* contributions. However, beyond low-order perturbation theory [17] it is difficult to disentangle the diagrammatic results. Specifically, the ladder diagrams in Fig. 1(a) contain intrinsic and side-jump contributions. Third order skew-scattering diagrams are collected in Fig. 1(b). Due to the vanishing of σ_{yx}^{II} in our model, all contributions to the AHE come from the Fermi surface, while in general (see, e.g., Ref. [18]) the Berry-phase contribution is associated with the entire Fermi volume.

The skew-scattering diagrams collected in Fig. 1(b) dominate for strong spin-orbit coupling $\epsilon_{so} \gg \epsilon_J, \epsilon_V$ where

$$\sigma_{yx}^{I,s} \approx \sigma_{yx}^{I,l} \frac{\epsilon_{so}(\epsilon_V^4 - \epsilon_J^4)}{4\epsilon_J^2 \epsilon_V (\epsilon_V^2 + 3\epsilon_J^2)}. \quad (9)$$

Here, we introduced the energy scale $\epsilon_V \equiv n_i V$, which measures the potential disorder strength. By contrast, for weaker spin-orbit coupling $\epsilon_{so} \ll \epsilon_J, \epsilon_V$, skew scattering and the ladder contributions can be of similar order of magnitude. For this reason, our plots always refer to the sum $\sigma_{yx}^{I,l} + \sigma_{yx}^{I,s}$ cf. Figs. 2 and 3.

Small impurity magnetization.—In the Rashba model with pointlike disorder, the AHE vanishes in the absence of magnetic scattering when both subbands are occupied [9,11]. At small impurity magnetization we therefore expect that the anomalous Hall conductivity is proportional to the magnetization, i.e., to $\hbar = n_i J \langle S_z \rangle$. However, in our model this holds only for very small polarization of the impurity spins. This can be understood analytically from the small magnetization expansion (for classical spins)

$$\begin{aligned} \sigma_{yx}^{I,l} &\approx \frac{e^2 \langle S_z \rangle}{2\pi} \frac{16\epsilon_J^3}{S} \left(\frac{\epsilon_V}{\epsilon_V^2 + \epsilon_J^2} - \frac{2\epsilon_J^2}{\epsilon_F(3\epsilon_V^2 + 7\epsilon_J^2)} \right), \\ \sigma_{yx}^{I,s} &\approx -\frac{e^2 \langle S_z \rangle}{2\pi} \frac{18\epsilon_{so}\epsilon_J(\epsilon_J^2 - \epsilon_V^2)}{S(7\epsilon_J^2 + 3\epsilon_V^2)^2}. \end{aligned} \quad (10)$$

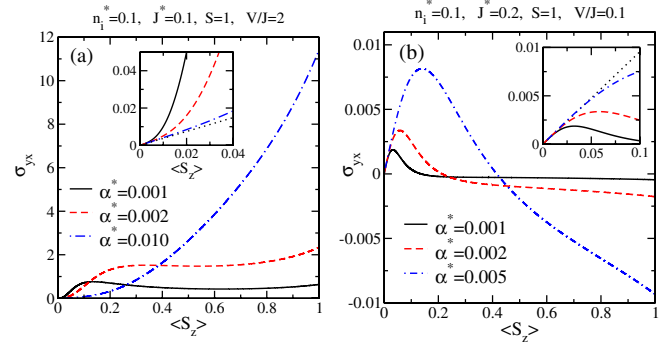


FIG. 2 (color online). Anomalous Hall conductivity for quantum spins with $S = 1$ as a function of the polarization of the impurity spins $\langle S_z \rangle$. The insets display zoom-ins for small $\langle S_z \rangle$, where the dotted lines indicate the α -independent slope. All conductivities are plotted in units of $e^2/(2\pi)$, using dimensionless units of the form $n_i^* = n_i/k_F^2$, $m^* = 1/2$, $J^* = 2mJ/\hbar^2$, $V^* = 2mV/\hbar^2$, $\alpha^* = 2m\alpha/(\hbar^2 k_F)$.

Note that a nonzero exchange coupling J is required for a nonvanishing AHE. Moreover, since the skew-scattering contribution $\sigma_{yx}^{I,s}$ is negligible for $\epsilon_{so} \ll \epsilon_J, \epsilon_V$, we obtain the remarkable result that in this limit, the slope of the anomalous Hall conductivity becomes approximately *independent* of the magnitude α of the spin-orbit interaction. Since a finite spin-orbit coupling is required for the existence of the AHE in the first place, this implies that the regime over which the linear magnetization dependence holds must shrink with decreasing spin-orbit coupling α , entailing a strongly nonlinear behavior of the anomalous Hall conductivity vs polarization of the impurity spins $\langle S_z \rangle$, as illustrated in Fig. 2.

Remarkably, we find that the AHE can even change sign as a function of impurity magnetization [see Fig. 2(b)]. This behavior is reminiscent of sign changes found experimentally in other systems [18,19]. Inspecting the expres-

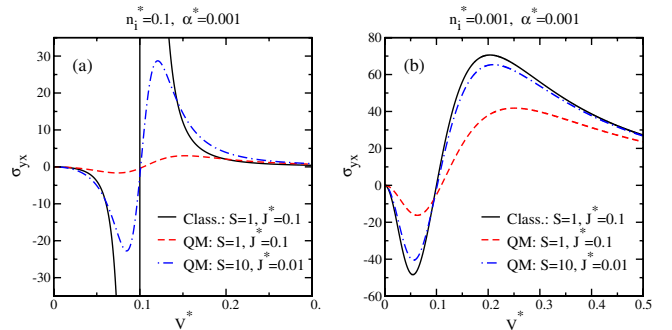


FIG. 3 (color online). Fully spin-polarized $\langle S_z \rangle = S$ anomalous Hall conductivity for classical $S = 1$ spins (solid lines) and quantum spins (dashed and dashed-dotted lines) for constant α^* , n_i^* , and J^* as a function of V^* . Panel (a) shows the limit $\epsilon_J \gg \Delta_{so}$ and (b) the limit $\epsilon_{so} \ll \epsilon_J \ll \Delta_{so}$. All conductivities are plotted in units of $e^2/(2\pi)$, using the dimensionless units of Fig. 2.

sions for the slope [Eq. (10)] and for the conductivity at maximal spin polarization $\langle S_z \rangle = S$ [Eq. (12) below], we find that for $\epsilon_{so} \ll \epsilon_J, \epsilon_V$, where the skew-scattering contribution to the slope is negligible, the conductivity as a function of $\langle S_z \rangle$ changes sign for scalar impurity potentials V of intermediate strength, i.e., for $JS > V > JS \frac{\epsilon_V}{\epsilon_F} \times \frac{2\epsilon_V^2 + 2\epsilon_J^2}{3\epsilon_V^2 + 7\epsilon_J^2}$. Note also that the overall sign of the AHE depends on the sign of the exchange coupling J .

Large impurity magnetization.—The most intriguing behavior of the anomalous Hall conductivity occurs in the limit where the impurity spins are near full polarization, i.e., for $\langle S_z \rangle \simeq S$. We first focus on the regime of weak spin-orbit coupling $\Delta_{so} \ll h = n_i J \langle S_z \rangle$ (i.e., $\lambda_F = \sqrt{h^2 + \alpha^2 k_F^2} \approx h$), where the scattering rate of the minority band

$$\Gamma_+ \approx \Gamma - \Gamma_z \frac{h}{\lambda_F} = \frac{n_i}{2} [V^2 - 2VJ \langle S_z \rangle \frac{h}{\lambda_F} + J^2 S(S+1)] \quad (11)$$

vanishes at $V = JS$ for classical spins. This absence of scattering arises from *interference* between the potential and magnetic components of the impurity potential and implies a *divergence* of the anomalous Hall conductivity. Note that this absence of scattering holds for minority spins only. For the majority band, Γ_- is *enhanced* due to the opposite sign of the interference term $\propto \Gamma_z$ [see Eq. (5)].

Indeed, near $\langle S_z \rangle \simeq S$ the anomalous Hall conductivity for classical spins in the regime $\Gamma \ll \epsilon_J, \epsilon_V$ reads

$$\sigma_{yx}^{I,I} \approx \frac{e^2}{2\pi} \frac{4\epsilon_{so}\epsilon_F^2\epsilon_V^2(\epsilon_J^2 + \epsilon_V^2)}{\epsilon_J(\epsilon_V^2 - \epsilon_J^2)^3}, \quad \frac{\sigma_{yx}^{I,S}}{\sigma_{yx}^{I,I}} \approx \frac{2\epsilon_J^2}{\epsilon_J^2 + \epsilon_V^2}. \quad (12)$$

This expression obviously diverges for $\epsilon_V = \epsilon_J$ and also implies a *sign change* of the anomalous Hall conductivity at $\epsilon_V = \epsilon_J$. For quantum spins the true divergence is eliminated. Nevertheless, a strong enhancement of the AHE is predicted at full spin polarization for $\epsilon_V \approx \epsilon_J$. As expected, the result for quantum spins approaches the classical divergence as the spin increases (see Fig. 3).

In addition, the divergence in the approximate expression, Eq. (12), is also cut off by a finite spin-orbit coupling α . However, the AHE remains strongly enhanced near full polarization $\langle S_z \rangle = S$ even when $\epsilon_{so} \ll \epsilon_J \ll \Delta_{so}$. In this regime of strong spin-orbit scattering, we obtain

$$\sigma_{yx}^{I,I} \approx \frac{e^2}{2\pi} \frac{4\epsilon_J^3\epsilon_V^2(\epsilon_V^2 - \epsilon_J^2)}{\epsilon_{so}(\epsilon_V^2 + \epsilon_J^2)^2(\epsilon_V^2 + 3\epsilon_J^2)}, \quad \frac{\sigma_{yx}^{I,S}}{\sigma_{yx}^{I,I}} \approx \frac{2\epsilon_J^2}{\epsilon_V^2 + 3\epsilon_J^2} \quad (13)$$

for classical spins. Obviously, the true divergence of the anomalous Hall conductivity at $\epsilon_V = \epsilon_J$ is replaced by a pronounced maximum of the anomalous Hall conductivity at $\epsilon_V \approx 2.2\epsilon_J$ as can be seen in Fig. 3(b) (solid line). Again quantum spins behave very similarly, and the classical result is recovered for large spins. Interestingly, for fully polarized quantum spins, $\langle S_z \rangle = S$, the anomalous Hall

conductivity becomes maximal in the crossover regime between the two limits discussed above, i.e., for $\epsilon_J \approx \Delta_{so}$.

Conclusions.—We have investigated the effects of magnetic impurities on the anomalous Hall effect and uncovered rich and unexpected behavior of the anomalous Hall conductivity. We find a highly nonlinear dependence on the spin magnetization and sign changes of the AHE as function of magnetization, as well as a resonant enhancement due to interference between potential and magnetic scattering from the magnetic impurities.

Although our work is motivated by the ubiquitous presence of magnetic impurities in spintronics materials, we have focused here on a thorough theoretical analysis of a simple model system, namely, a two-dimensional electron system with Rashba spin-orbit coupling. A more realistic description of the band structure of real spintronics materials remains an important task for future research. Indeed, recent experimental work [19] on the diluted magnetic semiconductor (In,Mn)Sb exhibits an intriguing sign change of the anomalous Hall conductivity as function of the impurity magnetization, which is interpreted in terms of the Berry-phase contribution to the AHE [18]. Our work shows that the occurrence of such sign changes is much more generic and a conclusive interpretation of the experimental data must await more detailed research.

This work was supported by a MÖB-DAAD grant, DIP, as well as SPP 1285 of the DFG. G. Z. has been supported by the Hungarian grants No. OTKA T046303 and No. NF061726.

-
- [1] R. Karplus and J. Luttinger, Phys. Rev. **95**, 1154 (1954).
 - [2] J. Smit, Physica (Amsterdam) **21**, 877 (1955).
 - [3] L. Berger, Phys. Rev. B **2**, 4559 (1970).
 - [4] For a recent review see P. Wölfle and K. A. Muttalib, Ann. Phys. (N.Y.) **15**, 508 (2006).
 - [5] D. Culcer, A. MacDonald, and Q. Niu, Phys. Rev. B **68**, 045327 (2003).
 - [6] V. K. Dugaev *et al.*, Phys. Rev. B **71**, 224423 (2005).
 - [7] N. A. Sinitsyn *et al.*, Phys. Rev. B **72**, 045346 (2005).
 - [8] S. Onoda, N. Sugimoto, and N. Nagaosa, Phys. Rev. Lett. **97**, 126602 (2006).
 - [9] J.-i. Inoue *et al.*, Phys. Rev. Lett. **97**, 046604 (2006); T. Kato *et al.*, New J. Phys. **9**, 350 (2007).
 - [10] M. F. Borunda *et al.*, Phys. Rev. Lett. **99**, 066604 (2007).
 - [11] T. S. Nunner *et al.*, Phys. Rev. B **76**, 235312 (2007).
 - [12] A. Fert and A. Friederich, Phys. Rev. B **13**, 397 (1976).
 - [13] I. Smorchkova and N. Samarth, Appl. Phys. Lett. **69**, 1640 (1996).
 - [14] J. Cumings *et al.*, Phys. Rev. Lett. **96**, 196404 (2006).
 - [15] P. Streda, J. Phys. C **15**, L717 (1982).
 - [16] A. Crépieux and P. Bruno, Phys. Rev. B **64**, 014416 (2001).
 - [17] N. A. Sinitsyn *et al.*, Phys. Rev. B **75**, 045315 (2007).
 - [18] T. Jungwirth, Q. Niu, and A. H. MacDonald, Phys. Rev. Lett. **88**, 207208 (2002).
 - [19] G. Mihály *et al.*, Phys. Rev. Lett. **100**, 107201 (2008).